# The Electrochemical Behaviour of Magnetocaloric Alloys La(Fe,Mn,Si)$_{13}$H$_x$ under Magnetic Field Conditions

Liya Guo,*[a] Edmund Lovell[b], Neil Wilson[c], Paul Burdett[c], Lesley F. Cohen[b] and Mary P. Ryan*[a]

[a] Department of Materials, Imperial College London, London, SW7 2AZ, UK

[b] Blackett Laboratory, Imperial College London, London, SW7 2AZ, UK

[c] Camfridge Ltd., Unit B1, Copley Hill Business Park, Cambridge, CB22 3GN, UK

*Abstract*

*The degradation mechanism of La(Fe,Mn,Si)$_{13}$H$_x$ has been examined under conditions representative of the complex operating parameters of a refrigeration cycle. The magnetic field effects are found to be dominated by magneto-transport and are most significant when the material is in its paramagnetic state – resulting in significantly accelerated corrosion rates.*

The magnetocaloric effect (MCE)-based cooling technique is promising for a low carbon future.[1-3] MCE is manifest by a temperature change of a magnetic material in an applied magnetic field.[2, 3] At temperatures slightly above the Curie Temperature $T_C$, when a magnetic field is applied, the MCE alloy La(Fe,Si)$_{13}$ undergoes an itinerant electron metamagnetic (IEM) transition, from the paramagnetic to the ferromagnetic state, resulting in a 'giant MCE'.[1]

In an active magnetic regenerator (AMR) cycle, the thermal changes induced by these magnetic transitions transfer to a heat exchanger through a heat transfer fluid, commonly water.[4, 5] However, contact between the active alloy and water can result in severe corrosion under typical operating conditions.[2] Although there is some reported work on the basic electrochemical behaviour of $La(Fe,Si)_{13}$, there are no reports concerning the influence of magnetic field on the reactivity of the material.[6] In addition, previous work on this class of material was typically carried out in pure water where there was no Ohmic-loss control, or attempts to correct for the high solution-resistance, which might introduce artefacts in the measurements.

The application of magnetic field during electrochemical reactions can play a role in accelerating the processes due to introduction of the Lorentz force, also known as the magnetohydrodynamic (MHD) force in fluids.[7-13] The Lorentz force acts on charge-carrying elements moving in a magnetic field and is given by:

$$F_L = i \times B \qquad (1)$$

Where $F_L$ is the Lorentz force, $i$ is the current density and $B$ is the magnetic induction. Figure 1 is a schematic diagram showing how we have assigned parallel/perpendicular field in this study. In this experiment, when the magnetic flux is parallel to the electrode surface, the magnetic field is referred as a parallel field with respect to the electrode surface (the dominant electrochemical current is assumed perpendicular to this). When the magnetic flux is perpendicular to the electrode surface, the magnetic field is referred as a perpendicular field, *i.e.* the field is defined with respect to the sample.

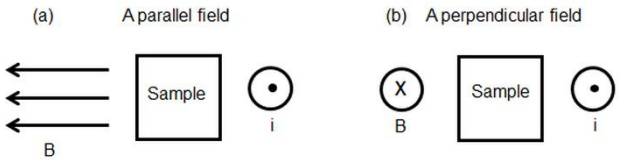


Figure 1 Schematic diagram showing a (a) parallel and (b) perpendicular magnetic field. i is the current density and B is the magnetic induction.

When a ferromagnetic electrode is placed within a magnetic field, the electrode will become magnetized. This will give rise to a second force: the field gradient force, and the magnetic flux adjacent to the electrode will deviate. Note that the field gradient force is negligible for electrodes in the paramagnetic state.[8]

In addition, under magnetic field cycling there is an associated magneto-volume change (1%-2% for the $La(Fe,Si)_{13}$ compounds) which could lead to local stresses, cracks and thus fracture of the brittle material.[5]

For the AMR cycle, there is usually a range of magnetocaloric alloys with a cascaded set of $T_C$ values.[14] Under an alternating changing magnetic field, depending on $T_C$, some alloys are paramagnetic and some remain ferromagnetic at a certain temperature. For some compounds, the IEM transition (magneto-volume changes) might take place as the field is changed. In addition, there will be sample spinning in practice, *i.e.* the orientation of compounds relative to the magnetic field direction changes. However, there are no reports concerning the influence of the magnetic field on the electrochemical and corrosion behaviour of $La(Fe,Si)_{13}$. The degradation of the material might in turn poison the giant MCE, reducing cooling efficiency and eventually stop the refrigerator working.[4] As a result, it is necessary to understand the alloy behaviour in the magnetocaloric system similar to the practical applications before commercialisation of these technologies is viable. In the present study, the effect of magnetic field direction, magnetic state of the material and magneto-volume change under an alternating changing field, were all considered.

As-received plates of $LaFe_{11.22}Mn_{0.46}Si_{1.33}H_x$ ($LFMSH_1$) and $LaFe_{11.28}Mn_{0.40}Si_{1.32}H_x$ ($LFMSH_2$) were studied. The $T_C$s of $LFMSH_1$ and $LFMSH_2$ are 281 K and 290 K (Figure 2) respectively. Therefore, $LFMSH_1$ samples are paramagnetic under all test conditions. $LFMSH_2$ samples are ferromagnetic when the test temperature is less than 290 K, with or without a 1.1 T magnetic field. For $LFMSH_2$, when the test temperature is between 290 K and 294 K, IEM transitions take place with a 1.1 T alternating changing field.

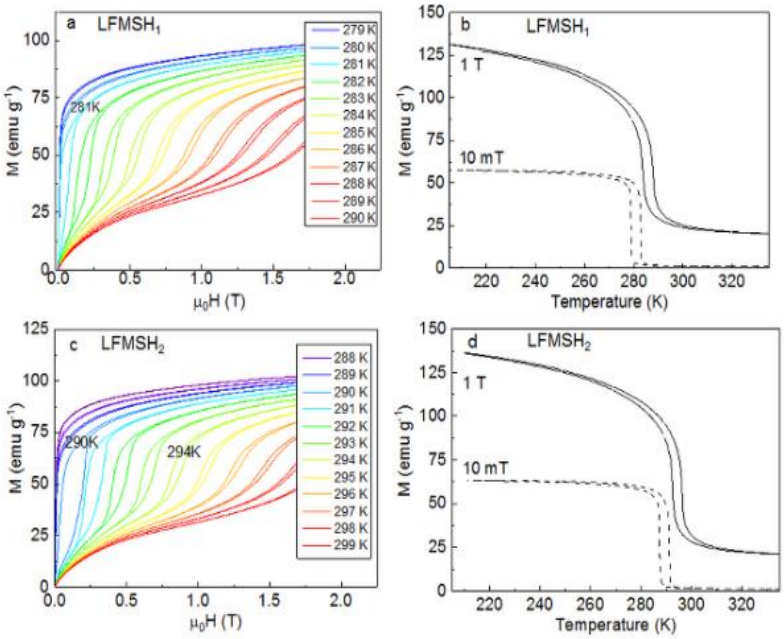


Figure 1 M (H) data (with a field sweep rate of 0.0017 T $s^{-1}$) of the magnetic transition of as-received (a) $LFMSH_1$ and (c) $LFMSH_2$ samples for a variety of temperatures around $T_C$. M (T) data (with a sweep rate of 0.0167 K $s^{-1}$) of the magnetic transition of as-received (b) $LFMSH_1$ and (d) $LFMSH_2$ samples in 1 T and 10 mT fields.

Potentiodynamic tests (Fig. S1, ESI†) were first carried out in the absence of a field to observe the general electrochemical behaviour, and to inform the choice of potentials to be applied in the potentiostatic tests. One *applied* potential giving cathodic current density, one *applied* potential (close to open circuit potential, OCP) giving low anodic current density, and one *applied* potential giving high anodic current density (representing severe corrosion rates)

were chosen to investigate the effect of magnetic field under various conditions (cathodic = 'inert', anodic low =active, and anodic high = accelerated). All electrochemical tests were carried out in a naturally-aerated pH-controlled non-interacting electrolyte (0.1 M $NaClO_4$, neutral) where Ohmic loss was minimised.

In our experiments the sample was moved in and out of the 1.1 T magnetic field to directly measure the effect of the field during electrochemical polarisation. A controlled test was first performed to investigate the effect of this movement on the current response in the absence of magnetic fields (Fig. S2, ESI†). The results show that the effect of linear movements on cathodic and low anodic polarization is negligible. Movement at high anodic polarization led to a small increase (<1%) in current densities. Corrosion products, which could hinder metal dissolution, might be mechanically removed during movement of the sample.[8, 15]

Figure 3 shows the response of current densities with or without constant magnetic fields in potentiostatic tests for paramagnetic ($LFMSH_1$) and ferromagnetic ($LFMSH_2$) samples. A summary of the data is also given (Table S1, ESI†). The sample was with a parallel field (red squares, 1.1 T), a perpendicular field (blue squares, 1.1 T) or no magnetic field (white squares). The change in current densities due to the application of a magnetic field (up to 60%) is much greater than the increase in current densities due to physical movement of the cell (less than 1%). Therefore, the effects shown in Figure 3 can be directly related to the magnetic field. Figures 3(a), (c) and (e) show the behaviour of $LFMSH_1$, which is paramagnetic under the test temperature: RT. Figures 3(b), (d) and (f) show the behaviour of $LFMSH_2$, which is ferromagnetic under the test conditions. The increasing (Figure 3(d))/decreasing (Figures 3(a) and (e)) tendency of current densities with time indicates that the electrochemical behaviour doesn't reach steady state within the period of the experiment.

However, we note that in the AMR cycle transient times will be on the scale of seconds and so the data do provide useful insights to the AMR system.

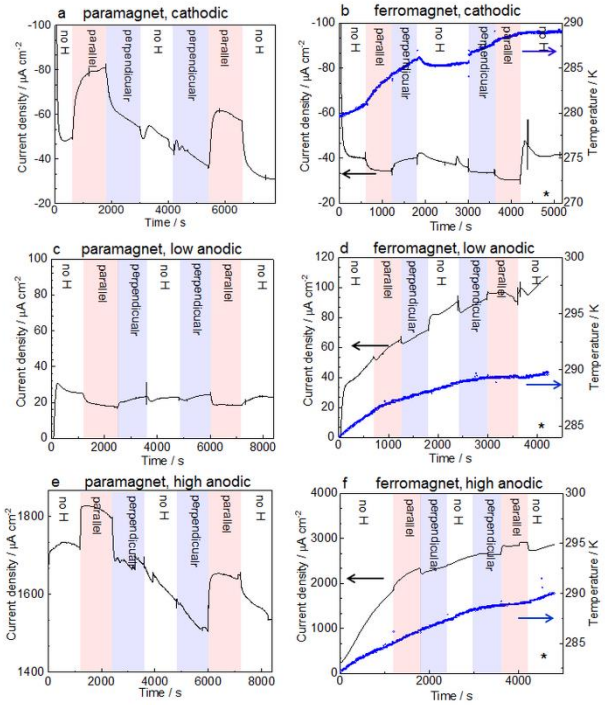


Figure 3 Sample $LFMSH_1$ was held at (a) -0.94V, followed by (c) -0.78 V and (e) -0.65 V; samples $LFMSH_2$ were held at (b) -0.94 V, (d) -0.72 V and (f) -0.57 V after immersion in solutions for 600 s without field at OCP. Tests were carried out in 0.1 M $NaClO_4$ with or without a constant parallel/perpendicular magnetic field (a), (c) and (e) at RT and (b), (d) and (f) at temperatures indicated in the figure. Tests (a), (c) and (e) were carried out on one sample and tests (b), (d) and (f) were carried out on three different samples. When there was thermally-induced magnetic transition, the block was labelled with '*'.

Figures 3(a), (c) and (e) show the Lorentz force induced enhancement in mass transport for a paramagnetic sample. The effect is most obvious with a parallel field (Equation 1), while it is negligible with a perpendicular field (with an applied potential, the current densities with a perpendicular field are similar to those with no field). Figure 3(a) clearly shows that at cathodic polarization, current densities are greatest when the sample is in a parallel field. In the studied condition, the cathodic reaction is dominated by oxygen reduction:

$$O_2 + 2H_2O + 4e^- \rightarrow 4OH^- \qquad (2)$$

At the studied potential, this reaction is a mixture of activation/electron-transfer and mass-transport control.[16,17] $F_L$, due to movement of charged-carriers ($Na^+$ and $ClO_4^-$ in the

electrolytes and $OH^-$ produced in the cathodic reactions), can enhance the mass transport in the system and its effects are therefore similar to rotating the electrode or stirring the solution.[18] $F_L$ is maximum with a parallel field. As a result, the MHD effect driven by $F_L$ accelerates the mass transport of the ionized species near the electrode surface. Consequently, the cathodic current densities are increased at the applied potential. The enhanced cathodic current with a parallel magnetic field is consistent with reported work where cathodic current increased with increasing rotating speed in rotating disc tests.[17, 19, 20]

The weight percentage of Fe is more than 70% in both materials (Table S2, ESI†). Therefore it is reasonable to simplify the anodic reaction/metal dissolution as following:

$$Fe \rightarrow Fe^{2+} + 2e^- \qquad (3)$$

With a small applied potential (Figure 3(c)), the corresponding net anodic current densities have a small negative contribution from oxygen reduction (cathodic current) and positive contribution from electrochemical metal dissolution (anodic current). For the above potential range studied, the anodic current is controlled by the electron-transfer step while the cathodic current is under mixed activation/mass-transport control.[21, 22] For neutral solutions, the effect of a magnetic field on electron-transfer step has generally been reported to be negligible while the cathodic current might be increased by a parallel magnetic field due to enhanced mass transport.[16, 23, 24] This gives rise to a decrease in the net anodic current when the applied potential is small. In addition, it has been proposed that with an increased mass transport, reactive solution species more easily reach the electrode surface and therefore a corrosion deposit/inhibitive layer is formed more easily.[9, 25] The formation of corrosion products: a mixture of oxides/hydroxides of silicon, manganese, iron and lanthanum (Fig. S3 and Table S3, ESI†) on the sample can block the electrode surface and thus decrease the corrosion

rates.[8, 15] Therefore, at the applied potential, the corresponding low anodic current densities are lowest with a parallel field.

With high dissolution rates, a large $F_L$ is expected (Equation 1) as well as the potential to form significant amounts of corrosion products (Fig. S3, ESI†). The stirring effect of $F_L$ can accelerate the removal of corrosion products and thus increase the corrosion rates. This is clearly demonstrated in Figure 3(e): at high anodic polarization, again the corrosion rates are greatest with a parallel field.

Figures 3(b), (d) and (f) illustrate the electrochemical behaviour of ferromagnetic samples $LFMSH_2$. The observations are consistent with combined effects of the field gradient force and $F_L$. When a ferromagnetic electrode is exposed to a magnetic field, the electrode will become magnetised and this will cause a deviation of the magnetic flux lines. The inhomogeneous flux density distribution gives rise to the field gradient force, distinct from $F_L$.[8,26,27]

Figure 3(b) illustrates that, for a ferromagnetic electrode, with the applied potential, the corresponding cathodic current densities are highest with no magnetic field and lowest with a parallel field. When the sample is initially immersed in the solution (at OCP, before cathodic polarisation), there might be metal dissolution and thus formation of corrosion products (Fig. S3(b), ESI†). The field gradient force attracts the dissolved paramagnetic $Fe^{2+}$ ions and oxygen to the periphery of the electrode surface (high field gradient), and this is followed by formation of corrosion products.[8, 27] Furthermore, in a parallel field, the MHD effect driven by $F_L$ accelerates the mass transport of reactive solution species to the electrode surface. Therefore, corrosion products form more easily with a parallel field and subsequently may hinder the cathodic reaction.

The inhibiting effect of the field gradient force is also observed in Figures 3(d) and (f). In Figure 3(d), the corresponding low anodic current densities of a ferromagnet are again the greatest without a magnetic field. In Figure 3(f) (heavily corroded), the increasing tendency in current densities of a sample with no field is greater than with a perpendicular field. However, when the anodic polarization is great and the corresponding anodic current densities are high, the Lorentz-induced MHD effects are significant enough to encourage accelerated metal dissolution. With high anodic polarization (Figure 3(f)), the dissolution rates with a parallel field are greater than with no field.

Figure 4 shows the response of low anodic current densities in potentiostatic tests when the sample is not in magnetic field or is in a changing (between zero and perpendicular) magnetic field at 1 Hz cycling frequency. At the test temperature, the IEM transition would take place with changing field (Figure 2). In this condition there is potential for micro-cracking, due to magneto-volume changes associated with the IEM transition: such effects would be expected to have an indicative current response.[28] In Figure 4, small fluctuations in current densities are observed when the sample is under a changing field. This might be caused by eddy currents. However, the figure clearly shows that the current densities under a changing magnetic field are not greater than those with no field. Compared with Figure 3, Figure 4 demonstrates that for short-term tests, the magneto-volume changes have a smaller impact than magnetohydrodynamic effects. It should be noted that the effect of magneto-volume changes (micro-cracks) associated with IEM transition on the corrosion behaviour was only assessed for short time scales and showed minimal effect. The material went through 2400 cycles in the present study while it is expected to undergo 50 to 500 million cycles for a commercial cooling device.[5] The accumulation of micro-cracks might lead to macro scale fracture eventually. The effect needs to be assessed in more detail in accelerated tests.

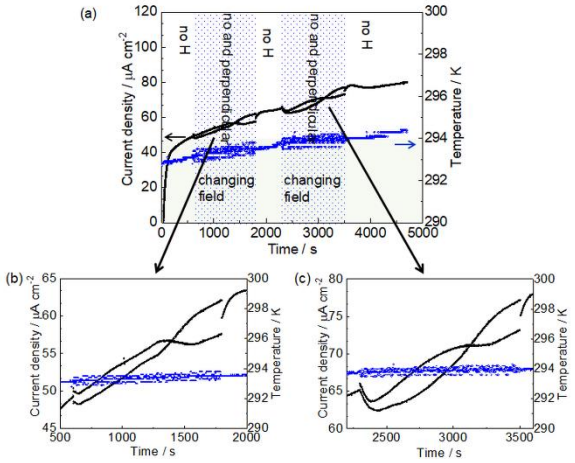

Figure 4 (a) The sample ($LFMSH_2$) was held at -0.735 V after immersion in the solution for 600 s without field at OCP. (b) and (c) time-zooms of figure (a). Tests were carried out in 0.1 M $NaClO_4$ with or without a changing magnetic field between no field and a 1.1 T perpendicular field at 1 Hz as indicated and at temperature shown in the figure.

In summary, magnetocaloric alloys $La(Fe,Mn,Si)_{13}H_x$ with two compositions were investigated in electrochemical tests in a naturally-aerated non-interacting electrolyte (0.1 M $NaClO_4$, neutral) with a 1.1 T magnetic field in both parallel and perpendicular directions to the electrode surface.

When the alloy was paramagnetic under the test conditions, the effect of a field perpendicular to the sample plate (parallel to the corrosion current direction) on the current densities was negligible. When the alloy was paramagnetic or ferromagnetic, the corrosion rate at low anodic polarizations (equivalent to ~0.3 mmpy) was greatest with no magnetic field and the corrosion rate at high anodic polarizations (equivalent to ~20.5 mmpy) was greatest with a parallel field. These observations are consistent with Lorentz force induced enhancement in mass transport, and the presence of the field gradient force for ferromagnets, which gives rise to an inhibiting effect.

The alloy was exposed in a changing magnetic field (at a frequency of 1 Hz) to investigate the effect of magneto-volume changes or micro-cracking on the anodic current response.

Compared with no field, there was no significant increase in current densities with a changing magnetic field. The long-term effects of micro-cracks which might eventually lead to fracture need to be further investigated in accelerated longer term tests.

Taken together these data suggest that in an active magnetic regenerator system, the electrochemical behaviour of the magnetocaloric alloys will be significantly different depending on the $T_C$ of the specific material and the orientation of the alloy in the field. The protocols used in the current work allow accurate assessments of the new energy material and future protection methods in the complex dynamic operating systems, and thus help optimise the system performance.

This work was funded by the EPSRC/Innovate UK programmes (EP/P511109/1 and 102741 respectively, and EP/P030548/1). MPR currently holds the RAEng/Shell Chair for Interfacial Nanoscience. The authors would like to thank Dr Alessandro Pastore from Camfridge Ltd., Dr Natasha Conway, Dr Graham Anderson and Dr Antonio D'Ammaro from Beko, and Dr Gareth Hinds from National Physical Laboratory for useful discussions.

**Conflicts of interest**

There are no conflicts to declare.

**Notes and References**

1. A.Fujita, S. Fujieda, Y. Hasegawa and K. Fukamichi, *Phys. Rev. B*, 2003, **67**, 12.
2. M. Balli, S. Jandl, P. Fournier and A. Kedous-Lebouc, *Appl. Phys. Rev.*, 2017, **4**, 27.
3. J. Lyubina, *J. Phys. D-Appl. Phys.*, 2017, **50**, 28.
4. S. Fujieda, K. Fukamichi and S. Suzuki, *J. Alloy. Compd.*, 2014, **600**, 67-70.
5. K. A. Gschneidner and V. K. Pecharsky, *International Journal of Refrigeration-Revue Internationale Du Froid*, 2008, **31**, 945-961.
6. M. Zhang, Y. Long, R.-c. Ye and Y.-q. Chang, *J. Alloy. Compd.*, 2011, **509**, 3627-3631.
7. O. Aaboubi, J. P. Chopart, J. Douglade, A. Olivier, C. Gabrielli and B. Tribollet, *J. Electrochem. Soc.*, 1990, **137**, 1796-1804.

8. Y. C. Tang and A. J. Davenport, *J. Electrochem. Soc.*, 2007, **154**, C362-C370.
9. X. J. Li, M. Zhang, B. Y. Yuan, L. Li and C. Wang, *Electrochim. Acta*, 2016, **222**, 619-626.
10. S. S. W. Yee and S. A. Bradford, *Am. Soc. Testing and Mater.*, 1992, **1148**, 90-101.
11. N. Leventis and A. Dass, *J. Am. Chem. Soc.*, 2005, **127**, 4988-4989.
12. S. Ling, Y. Jia, F. Ning, H. Li, Q. Xiao and Z. Lu, *Electrochem. Soc. Trans.*, 2018, **85**, 615-623.
13. T. Z. Fahidy, *J. Appl. Electrochem.*, 1983, **13,** 553-563.
14. M. Balli, O. Sari, L. Zamni, C. Mahmed and J. Forchelet, *Mater. Sci. Eng. B-Adv. Funct. Solid-State Mater.*, 2012, **177**, 629-634.
15. R. Sueptitz, K. Tschulik, M. Uhlemann, J. Eckert and A. Gebert, *Mater. Corrosion*, 2014, **65**, 803-808.
16. K. Shinohara, K. Hashimoto and R. Aogaki, *Chemistry Letters*, 2002, **31**, 738-739.
17. N. G. Smart, M. L. Hitchman, R. O. Ansell and J. D. Fortune, *Corrosion Sci.*, 1994, **36**, 1473-1489.
18. G. Hinds, F. E. Spada, J. M. D. Coey, T. R. N. Mhiochain and M. E. G. Lyons, *J. Phys. Chem. B*, 2001, **105**, 9487-9502.
19. B. T. Ellison and I. Cornet, *J. Electrochem. Soc.*, 1971, **118**, 68-72.
20. S. Jiang, F. Chai, H. Su and C. F. Yang, *Corrosion Sci.*, 2017, **123**, 217-227.
21. Z. Lu, D. Huang, W. Yang and J. Congleton, *Corrosion Sci.*, 2003, **45**, 2233-2249.
22. Z. P. Lu and W. Yang, *Corrosion Sci.*, 2008, **50**, 510-522.
23. J. Hu, S. Fu, Y. Huo, Y. Long and J. N. Xue, *J. Rare Earths*, 2016, **34**, 283-287.
24. F. M. F. Rhen, G. Hinds and J. M. D. Coey, *Electrochemistry Communications*, 2004, **6**, 413-416.
25. B. R. Tian and Y. F. Cheng, *Corrosion Sci.*, 2008, **50**, 773-779.
26. M. D. Pullins, K. M. Grant, H. S. White, *J. Phys. Chem. B*, 2001, **105,** 8989-8994.
27. R. Sueptitz, J. Koza, M. Uhlemann, A. Gebert and L. Schultz, *Electrochim. Acta*, 2009, **54**, 2229-2233.
28. S. T. Zhou, A, *Corrosion*, 2006, **62**, 508-513.